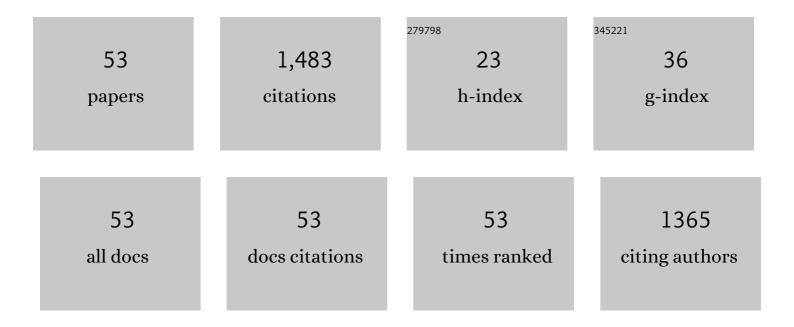
## Liqiang Zhang

List of Publications by Year in descending order

Source: https://exaly.com/author-pdf/4395073/publications.pdf Version: 2024-02-01



μοιλής Ζηλής

#	Article	IF	CITATIONS
1	DS <sup>4</sup> L: Deep Semisupervised Shared Subspace Learning for Hyperspectral Image Classification. IEEE Transactions on Geoscience and Remote Sensing, 2022, 60, 1-14.	6.3	3
2	Ambient temperatures associated with increased risk of motor vehicle crashes in New York and Chicago. Science of the Total Environment, 2022, 830, 154731.	8.0	7
3	DSL-BC: Deep Subspace Learning With Boundary Consistency for Hyperspectral Image Classification. IEEE Transactions on Geoscience and Remote Sensing, 2022, 60, 1-14.	6.3	1
4	DRFL-VAT: Deep Representative Feature Learning With Virtual Adversarial Training for Semisupervised Classification of Hyperspectral Image. IEEE Transactions on Geoscience and Remote Sensing, 2022, 60, 1-14.	6.3	3
5	A Dense Feature Pyramid Network-Based Deep Learning Model for Road Marking Instance Segmentation Using MLS Point Clouds. IEEE Transactions on Geoscience and Remote Sensing, 2021, 59, 784-800.	6.3	27
6	Hierarchical Aggregated Deep Features for ALS Point Cloud Classification. IEEE Transactions on Geoscience and Remote Sensing, 2021, 59, 1686-1699.	6.3	12
7	SLCRF: Subspace Learning With Conditional Random Field for Hyperspectral Image Classification. IEEE Transactions on Geoscience and Remote Sensing, 2021, 59, 4203-4217.	6.3	7
8	Land-Use Mapping for High-Spatial Resolution Remote Sensing Image Via Deep Learning: A Review. IEEE Journal of Selected Topics in Applied Earth Observations and Remote Sensing, 2021, 14, 5372-5391.	4.9	25
9	Relationship between Air Pollutant Exposure and Gynecologic Cancer Risk. International Journal of Environmental Research and Public Health, 2021, 18, 5353.	2.6	13
10	Evaluation of county-level poverty alleviation progress by deep learning and satellite observations. Big Earth Data, 2021, 5, 576-592.	4.4	5
11	MLRSNet: A multi-label high spatial resolution remote sensing dataset for semantic scene understanding. ISPRS Journal of Photogrammetry and Remote Sensing, 2020, 169, 337-350.	11.1	60
12	DML-GANR: Deep Metric Learning With Generative Adversarial Network Regularization for High Spatial Resolution Remote Sensing Image Retrieval. IEEE Transactions on Geoscience and Remote Sensing, 2020, 58, 8888-8904.	6.3	24
13	Latent Relationship Guided Stacked Sparse Autoencoder for Hyperspectral Imagery Classification. IEEE Transactions on Geoscience and Remote Sensing, 2020, 58, 3711-3725.	6.3	19
14	Air pollution exposure associates with increased risk of neonatal jaundice. Nature Communications, 2019, 10, 3741.	12.8	48
15	Air pollution-induced missed abortion risk for pregnancies. Nature Sustainability, 2019, 2, 1011-1017.	23.7	50
16	A Flexible Architecture for Extracting Metro Tunnel Cross Sections from Terrestrial Laser Scanning Point Clouds. Remote Sensing, 2019, 11, 297.	4.0	28
17	PSASL: Pixel-Level and Superpixel-Level Aware Subspace Learning for Hyperspectral Image Classification. IEEE Transactions on Geoscience and Remote Sensing, 2019, 57, 4278-4293.	6.3	22
18	Self-Supervised Feature Learning With CRF Embedding for Hyperspectral Image Classification. IEEE Transactions on Geoscience and Remote Sensing, 2019, 57, 2628-2642.	6.3	35

LIQIANG ZHANG

#	Article	IF	CITATIONS
19	Joint Discriminative Dictionary and Classifier Learning for ALS Point Cloud Classification. IEEE Transactions on Geoscience and Remote Sensing, 2018, 56, 524-538.	6.3	16
20	Large-scale urban point cloud labeling and reconstruction. ISPRS Journal of Photogrammetry and Remote Sensing, 2018, 138, 86-100.	11.1	49
21	A Deep Neural Network With Spatial Pooling (DNNSP) for 3-D Point Cloud Classification. IEEE Transactions on Geoscience and Remote Sensing, 2018, 56, 4594-4604.	6.3	42
22	Projection learning with local and global consistency constraints for scene classification. ISPRS Journal of Photogrammetry and Remote Sensing, 2018, 144, 202-216.	11.1	9
23	Self-Supervised Low-Rank Representation (SSLRR) for Hyperspectral Image Classification. IEEE Transactions on Geoscience and Remote Sensing, 2018, , 1-15.	6.3	31
24	Learning a Discriminative Distance Metric With Label Consistency for Scene Classification. IEEE Transactions on Geoscience and Remote Sensing, 2017, 55, 4427-4440.	6.3	28
25	A hierarchical methodology for urban facade parsing from TLS point clouds. ISPRS Journal of Photogrammetry and Remote Sensing, 2017, 123, 75-93.	11.1	36
26	Classification of Urban Point Clouds: A Robust Supervised Approach With Automatically Generating Training Data. IEEE Journal of Selected Topics in Applied Earth Observations and Remote Sensing, 2017, 10, 1207-1220.	4.9	24
27	A feature extraction and similarity metric-learning framework for urban model retrieval. International Journal of Geographical Information Science, 2017, 31, 1749-1769.	4.8	1
28	3DCNN-DQN-RNN: A Deep Reinforcement Learning Framework for Semantic Parsing of Large-Scale 3D Point Clouds. , 2017, , .		49
29	Discriminative-Dictionary-Learning-Based Multilevel Point-Cluster Features for ALS Point-Cloud Classification. IEEE Transactions on Geoscience and Remote Sensing, 2016, 54, 7309-7322.	6.3	34
30	A Three-Step Approach for TLS Point Cloud Classification. IEEE Transactions on Geoscience and Remote Sensing, 2016, 54, 5412-5424.	6.3	44
31	A Three-Layered Graph-Based Learning Approach for Remote Sensing Image Retrieval. IEEE Transactions on Geoscience and Remote Sensing, 2016, 54, 6020-6034.	6.3	72
32	A Multilevel Point-Cluster-Based Discriminative Feature for ALS Point Cloud Classification. IEEE Transactions on Geoscience and Remote Sensing, 2016, 54, 3309-3321.	6.3	81
33	A Multiscale and Hierarchical Feature Extraction Method for Terrestrial Laser Scanning Point Cloud Classification. IEEE Transactions on Geoscience and Remote Sensing, 2015, 53, 2409-2425.	6.3	138
34	A Gestalt rules and graph-cut-based simplification framework for urban building models. International Journal of Applied Earth Observation and Geoinformation, 2015, 35, 247-258.	2.8	14
35	Continuous Extraction of Subway Tunnel Cross Sections Based on Terrestrial Point Clouds. Remote Sensing, 2014, 6, 857-879.	4.0	49
36	A Methodology for Automated Segmentation and Reconstruction of Urban 3-D Buildings from ALS Point Clouds. IEEE Journal of Selected Topics in Applied Earth Observations and Remote Sensing, 2014, 7, 4199-4217.	4.9	106

LIQIANG ZHANG

#	Article	IF	CITATIONS
37	An Optimized BaySAC Algorithm for Efficient Fitting of Primitives in Point Clouds. IEEE Geoscience and Remote Sensing Letters, 2014, 11, 1096-1100.	3.1	14
38	A mathematical morphology-based multi-level filter of LiDAR data for generating DTMs. Science China Information Sciences, 2013, 56, 1-14.	4.3	17
39	Perception-based shape retrieval for 3D building models. ISPRS Journal of Photogrammetry and Remote Sensing, 2013, 75, 76-91.	11.1	18
40	Variational retrieval of leaf area index from MODIS time series data: examples from the Heihe river basin, north-west China. International Journal of Remote Sensing, 2012, 33, 730-745.	2.9	11
41	Urban building roof segmentation from airborne lidar point clouds. International Journal of Remote Sensing, 2012, 33, 6497-6515.	2.9	60
42	Automatic simplification and visualization of 3D urban building models. International Journal of Applied Earth Observation and Geoinformation, 2012, 18, 222-231.	2.8	26
43	A geometry and texture coupled flexible generalization of urban building models. ISPRS Journal of Photogrammetry and Remote Sensing, 2012, 70, 1-14.	11.1	13
44	Transmission and visualization of large geographical maps. ISPRS Journal of Photogrammetry and Remote Sensing, 2011, 66, 73-80.	11.1	10
45	Interactive visualization of multi-resolution urban building models considering spatial cognition. International Journal of Geographical Information Science, 2011, 25, 5-24.	4.8	19
46	An efficient rendering method for large vector data on large terrain models. Science China Information Sciences, 2010, 53, 1122-1129.	4.3	15
47	An improved line-of-sight method for visibility analysis in 3D complex landscapes. Science China Information Sciences, 2010, 53, 2185-2194.	4.3	20
48	Adaptive multi-resolution labeling in virtual landscapes. International Journal of Geographical Information Science, 2010, 24, 949-964.	4.8	6
49	Web-based terrain and vector maps visualization for Wenchuan earthquake. International Journal of Applied Earth Observation and Geoinformation, 2010, 12, 439-447.	2.8	7
50	Web-based visualization of spatial objects in 3DGIS. Science in China Series F: Information Sciences, 2009, 52, 1588-1597.	1.1	6
51	Visualization of large spatial data in networking environments. Computers and Geosciences, 2007, 33, 1130-1139.	4.2	15
52	Effective solutions to a global 3D visual system in networking environments. Science in China Series D: Earth Sciences, 2005, 48, 2032-2039.	0.9	7
53	A web-mapping system for real-time visualization of the global terrain. Computers and Geosciences, 2005, 31, 343-352.	4.2	7